

Synthesis, characterization and ferroelectric properties of lead-free $K_{0.5}Na_{0.5}NbO_3$ nanotube arrays

Di Zhou (周迪),^{1,2} Haoshuang Gu (顾豪爽),^{2,a)} Yongming Hu (胡永明),^{1,2} Huyong Tian (田虎永),^{2,3} Zhao Wang (王钊),² Zheli Qian (钱哲理),² and Yu Wang (王雨)^{1,b)}

¹Department of Applied Physics and Materials Research Center, The Hong Kong Polytechnic University, Hong Kong SAR, China

²Key Lab of Ferro- and Piezoelectric Materials and Devices of Hubei Province, Faculty of Physics and Electronic Technology, Hubei University, Wuhan 430062, China

³Department of Imaging and Applied Physics, Curtin University of Technology, Washington, Australia

(Received 20 December 2010; accepted 23 April 2011; published online 3 June 2011)

Lead-free $K_{0.5}Na_{0.5}NbO_3$ (KNN) nanotube arrays were synthesized by a sol-gel method with anodic aluminum oxide templates. The obtained KNN nanotubes exhibited a polycrystalline and monoclinic perovskite structure with diameters of ~ 200 nm and wall thickness of ~ 30 – 40 nm, respectively. The polarization-electric loop curve of the nanotubes array were examined showing the values of $2P_r$ and $2E_c$ at about $3.4 \mu\text{C}/\text{cm}^2$ and $13 \text{ kV}/\text{cm}$, respectively, under a maximum electric field of $12.5 \text{ kV}/\text{cm}$. The piezoelectric characteristics of individual KNN nanotube array was also identified through piezoresponse force microscopy. © 2011 American Institute of Physics. [doi:10.1063/1.3592636]

I. INTRODUCTION

The use of lead-free ferro- and piezo-electric materials has gained much attention in recent years. Sodium potassium niobate ($K_xNa_{1-x}NbO_3$), a promising candidate for replacing $Pb(Zr_xTi_{1-x})O_3$ (PZT) in piezoelectric devices as a lead-free material, is appealing for potential piezoelectric applications because of its relatively low dielectric permittivity, high electro-mechanical coupling coefficient as well as good nonlinear optical and electro-optical properties.^{1–4} $K_{0.5}Na_{0.5}NbO_3$ (KNN), a combination of ferroelectrics $KNbO_3$ and anti-ferroelectrics $NaNbO_3$, has been reported to possess good piezoelectric properties (as it is near the morphotropic phase boundary), moderate dielectric constant (ranging from 300 to 600) and relatively large piezoelectric coefficient (d_{33}) (~ 80 – $120 \text{ pC}/\text{N}$).⁵ Although the piezoelectric properties of (K,Na) NbO_3 ceramics are not as high as those of commercial PZT, (K,Na) NbO_3 ceramics can be used for several applications such as high frequency transducers, ultrasonic diagnostics and tunable microwave components.^{6–8} Over the past decade, most research activities concerning (K,Na) NbO_3 have focused on two areas: (1) to improve the material's sintering activity and (2) to enhance the ferro- and piezo-electric properties of KNN ceramics and thin films. For example, Bernard *et al.* reported that the KNN ceramics prepared in low-temperature condition could possess piezoelectric properties of d_{33} coefficient of $120 \text{ pC}/\text{N}$ and Zhou *et al.* described how to fabricate dense ceramics of Ta-doped KNN (KNTN) using refined nanopowders synthesized through hydrothermal method as start materials.^{9,10} Hu *et al.* has also reported the synthesis of $KTa_{0.25}Nb_{0.75}O_3$ and (K,Na) NbO_3 nanorods via orientation-control approaches.^{11,12} In another study, Ahn *et al.* examined the effects of K and Na excess on the ferroelectric and piezo-

electric properties of (K,Na) NbO_3 thin films, and the results showed that the optimized (K,Na) NbO_3 thin film showed good fatigue resistance with a piezoelectric constant of $40 \text{ pm}/\text{V}$, which is comparable to that of a polycrystalline PZT thin film.¹³ The effects of grains size on the dielectric response of KNN ceramics have also been studied by Buixaderas *et al.*¹⁴

With the rapid development of nanoscale technologies and devices, the properties exhibited in ferroelectric nanomaterials are quite different from those in bulk. For example, many ferroelectric properties, including the Curie temperature, mean polarization, area of hysteresis loop, coercive electric field, piezoelectric strain and remnant polarization, will become size dependent when certain dimensions are changed to nanoscale.¹⁵ Many of the ferroelectric nanostructures are potentially useful for applications related to microelectronics, biochemistry and environmental protections.^{16–18} Theoretical calculations of ferroelectrics with lower dimensionality have provided insights into how ferroelectric properties and size of nanowires are related to each other and how to select a suitable nanowire in terms of size for optimized performance.^{19,20} Therefore, the synthesis of 1D ferroelectric nanostructures is of great significance not only for fundamental understanding, but also for future applications.

Among the many synthesis methods, template-assisted synthesis has been widely employed to produce nanowire/tube arrays. In this method, the most commonly utilized templates are porous anodic aluminum oxide (AAO) and track-etched polycarbonate membranes. These templates have 1D nanoscale pores or channels in which a sol or an aqueous solution containing the desired components can be incorporated. In the following drying and annealing processes, the solvent evaporates and the material starts to densify and crystallize, forming 1D nanostructures whose dimensions can be precisely controlled by the pore diameter and the pore length of the templates.^{21–23} A number of studies concerning KNN films, ceramics and powders have been carried out in

^{a)}Electronic mail: guhsh583@yahoo.com.cn. Fax: (86) 27 88662960.

^{b)}Electronic mail: apywang@inet.polyu.edu.hk. Fax: (852) 23337629.

the past, yet little attention has been paid to KNN nanotubes so far. In this paper, we reported the synthesis of KNN nanotube arrays using the sol-gel method through commercially available AAO templates with pore diameters of ~ 200 nm. In addition, the morphologies and microstructures, phase as well as the ferroelectric and piezoelectric properties of the KNN nanotubes or/and arrays have been discussed.

II. EXPERIMENTAL DETAILS

The KNN nanotube arrays were synthesized by using a sol-gel process utilizing the AAO templates that are commercially available porous membranes (Whatman Anodisc 25) with a nominal pore diameter of 200 nm. The preparation of KNN precursor solution was conducted following the methods reported in the literature.^{24,25} The final concentration of precursor solution was adjusted to be 0.2 M by adding 2-methoxyethanol and acetic acid. The AAO templates were immersed into the precursor solution for 0.5 h under a lower atmospheric pressure condition. Then the templates containing the sol precursor were taken out of the solution and calcined in air at 700 °C for 0.5 h using a tube furnace.

The surface and cross-section morphologies of the KNN nanotube arrays were characterized by field emission scanning electron microscopy (FESEM, HITACHI, S-4800). The phase structures of the KNN nanotube array and KNN powders samples were carried out by an x-ray diffractometer (XRD, Bruker D8), using $\text{CuK}\alpha$ radiation ($\lambda = 1.5406 \text{ \AA}$) as the radiation source. The microstructure of a single KNN nanotube was examined through transmission electron microscopy (TEM, JEM 2010). For SEM and TEM observations, the alumina was removed by immersing the AAO/KNN arrays into a 4 M NaOH aqueous solution for a desired amount of time. To measure the ferroelectric properties of the KNN nanotube arrays, both surfaces of the array were first polished carefully with sand paper until the KNN nanotubes emerged before a layer of Au with a thickness of 100 nm was sputtered on both sides of the template as electrode. Then the polarization-electric (P - E) loop of the KNN nanotube array was measured by Sawyer-Tower method (frequency of the signal = 1 kHz). The piezoelectric properties of the KNN nanotube were studied by piezoresponse force microscopy (PFM, Nanoscope IV-Dimension 3100).

III. RESULTS AND DISCUSSION

The XRD patterns of as-prepared KNN nanotubes after removing the AAO template completely and KNN gel powders calcined under the same conditions are presented in Fig. 1. All diffraction peaks of KNN gel powders are well consistent with the standard powder XRD pattern of monoclinic perovskite structure with a symmetry of space group $Pm(6)$, and can be indexed according to the JCPDS card No. 77-0038. Analogously, a similar XRD pattern was observed from the KNN nanotube sample without extra peaks, suggesting that a pure polycrystalline perovskite structure of KNN was obtained without noticeable impurity phase. The results also show that the peak intensities of KNN nanotubes are much weaker and broader than those of the corresponding peaks of the powders because the amount of KNN

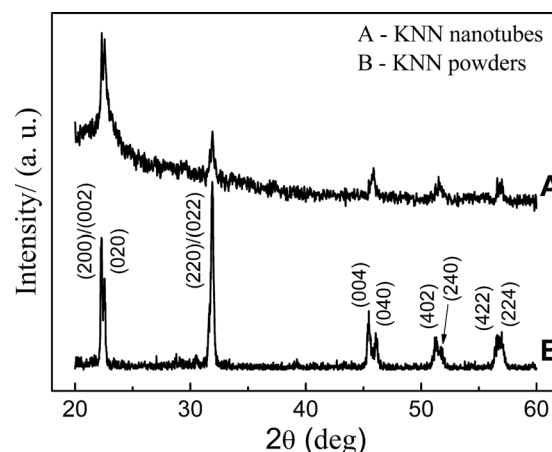


FIG. 1. XRD patterns of the KNN nanotube arrays and KNN powders derived from the same sol calcined at 700 °C.

particles consisted in nanotubes is very limited comparing with that in powders. On the other hand, the grain size effects may have contributed to the weaker and broader peaks of KNN nanotubes. Based on the Scherrer formula, the crystallite sizes were calculated using the data of three strongest diffractions (i.e., 200, 020 and 220 diffractions) and the values are ~ 54 nm for KNN gel powders and ~ 30 nm for KNN nanotubes, respectively. It is also worth noting that the relative intensity of the diffraction peaks of the KNN nanotubes has changed when compared to that of the powders. It is known that the (220) diffraction peak is the most intense for KNN ceramics while (200) diffraction peak is the most intense for the nanotubes sample, implying the KNN nanotubes have a preferred orientation. The lattice parameters of the KNN nanotubes and powders samples (calculated by MDI JADE5) are listed in Table I. The lattice parameters and volumes of nanotubes are slightly smaller than that of KNN powders, which is caused by the size-effect arisen from the nanoscale grains of KNN nanotubes.²⁶

Figure 2 presents the SEM images of the surface and cross-section morphologies of KNN nanotubes after removing the AAO templates partially. Figure 2(a) shows that there are large amounts of fiberlike products, which are uniformly distributed and parallel to each other. Meanwhile there is a certain degree of bundling at the top of the nanotubes. This may result from the condition in which the nanotubes are uncovered by the framework of the AAO templates and have become partly freestanding after the surface of AAO templates was dissolved. It can be conceived that the surface energy of the nanotubes has caused this interesting phenomenon. The inset of Fig. 2(a) shows clearly the hollow structures of fiberlike products. The tubular morphologies were further examined, which were marked with black arrows. As

TABLE I. Lattice parameters for KNN nanotubes and powders.

	$a/(\text{\AA})$	$b/(\text{\AA})$	$c/(\text{\AA})$	$\beta/(\text{^\circ})$	$V/(\text{\AA}^3)$
Powders	7.9913(4)	7.8734(5)	7.9651(4)	90.7039	501.12
Tubes	7.9629(9)	7.8696(3)	7.9390(8)	90.2313	497.50

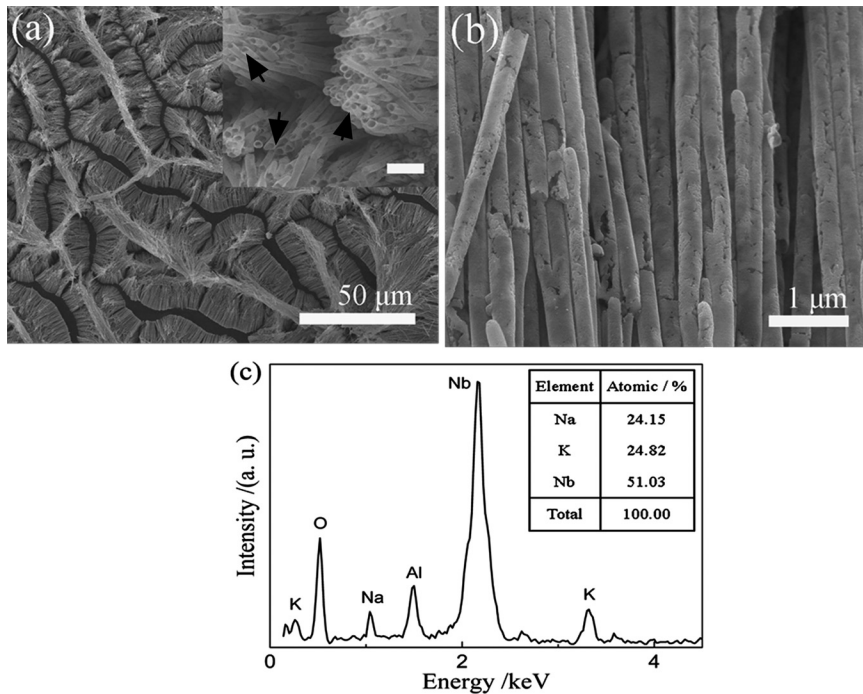


FIG. 2. SEM images of the KNN nanotubes after dissolving AAO template incompletely. (a) top view in low and high magnification (inset, the bar is 1 μm); (b) cross-section view; (c) EDX spectrum of the KNN nanotubes, inset: the atomic ratio of products.

shown in Fig. 2(b), the KNN nanotubes have outer diameters in the range of 200–250 nm, which are slightly larger than the pore diameters of templates employed. This could be attributed to the etching of the acidic KNN sol precursor to the AAO templates during the synthesis process; i.e., when the AAO templates were immersed into KNN sol precursor, the nanochannels of templates were expanded by the acidic solution. Figure 2(c) shows a representative energy-disperse x-ray (EDX) spectrum of the KNN nanotubes. It is clear that the nanotubes consist of Na, K and Nb (element Al comes from AAO template incompletely removed). The atomic ratio of these three elements is given in the inset of Fig. 2(c), showing that Na: K: Nb is approximate to 1: 1: 2. An ideal stoichiometric ratio of the as-prepared KNN nanotubes demonstrates that the sol-gel method offers advantages such as excellent compositional control and homogeneity at molecular level when synthesizing complex oxides.

The microstructure of the KNN nanotubes was further examined by TEM. An apparent hollow morphology was indicated with the transparency between the intermediary areas and edges of the rodlike samples, as shown in the Fig. 3(c). The thickness of the wall of nanotube is ~ 35 nm, which was marked in the Fig. 3(b), and the outer diameter of the nanotube is consistent with the measurement from SEM images. It is also evident that the individual KNN nanotube is straight but has a relatively rough and irregularly structured outer wall, implying the KNN nanotubes are composed of an amount of nano-particles with disordered arrangement. The inset of Fig. 3(a) shows a typical pattern of selected area electron diffraction (SAED) taken from a single KNN nanotube. The indexed ringlike patterns reveal the polycrystalline structure nature of the KNN nanotubes. Generally, the nanotubes/wires prepared by the sol-gel method within AAO templates are of polycrystalline structure. It should be noted that

the diffraction rings are discontinuous and consist of rather sharp spots, indicating the nanotubes are well crystallized.²⁷ The monoclinic perovskite structure of the KNN nanotubes was also verified by using a high-resolution transmission electron microscope (HRTEM), as shown in Fig. 3(d). It can be seen that the wall of the nanotubes is composed of randomly aligned nano-particles. In the HRTEM image, the diffraction fringes with a spacing of 0.408 nm correspond to the

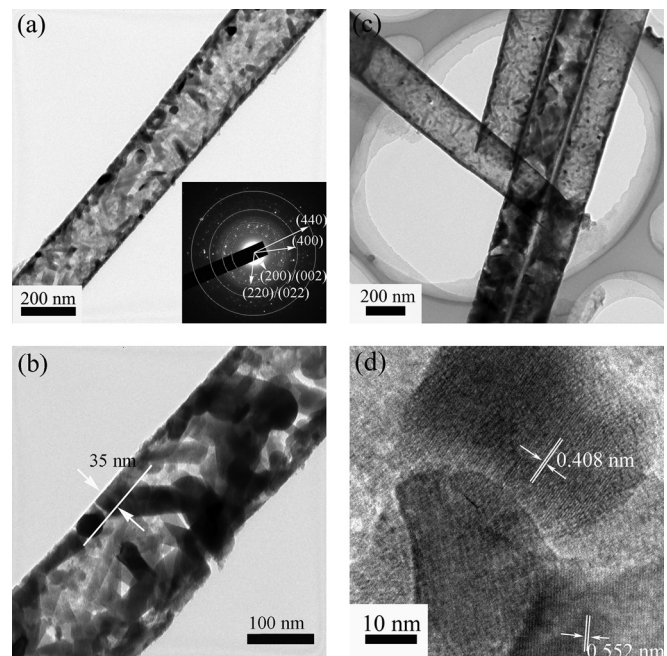


FIG. 3. (a)–(c) TEM images and SAED pattern [inset of Fig. 3(a)] of KNN nanotubes after completely dissolving AAO template; (d) HRTEM image of the KNN nanotube.

(200) planes while those with a spacing of 0.552 nm correspond to the (101) planes.

The dielectric and polarization properties of KNN films have been a major area of concern and a number of high ferroelectric performances of KNN films have been reported in the past.^{28–30} However, little has been reported on the relative ferroelectric or piezoelectric properties of KNN nanotubes. Figure 4(a) shows the P-E hysteresis loops of the KNN nanotube array measured with different voltage at room temperature while the schematic drawing of measurement configuration is shown in the inset. The hysteresis loops demonstrate clear room temperature ferroelectricity of the KNN nanotubes with some leakage current. The existence of leakage component could be attributed to a number of factors including defects of nano-structures, space charge and the interface conditions between nanowires and internal-wall of templates. One can also see that the remanent polarization ($2P_r$) and the coercive electric field ($2E_c$) obtained from the P-E hysteresis loops are about $3.4 \mu\text{C}/\text{cm}^2$ and 13 kV/cm under the applied voltage of 75 V, respectively. The values of P_r and E_c are much lower than those of sol-gel derived polycrystalline KNN films, which could be explained as following. First, there is an intrinsic size effect in low-dimensional ferroelectric materials. The typical phenomenon of such effect is the reduction of ferroelectricity with reducing grain sizes, which is often associated with

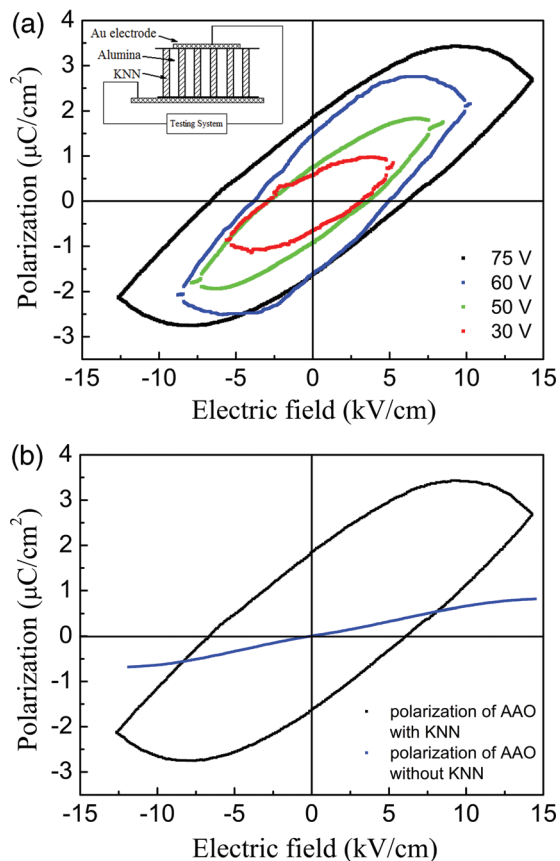


FIG. 4. (Color online) (a) P-E hysteresis loops of KNN nanotube arrays embedded in AAO template measured with different voltage; the inset is the schematic drawing of the measurement configuration; (b) P-E hysteresis loops of AAO template without KNN nanotubes and with nanotubes.

dielectric anomaly.^{31–33} Second, the geometry of the nanotube sample is also an important issue.³³ In this experiment, the measurement of ferroelectricity was made with a nanotube array embedded in AAO template with a relatively intricate field distribution. The actual measurements of hysteresis loops of AAO without KNN nanotubes and with nanotubes were presented, respectively, in Fig. 4(b). The hysteresis loop of AAO with KNN displays a co-effect consisting of polarization derived from KNN (ferroelectric polarization P_f) and AAO template (paraelectric polarization P_p), i.e., the measured polarization $P(E)$ could be described as an equation: $P(E) = P_f(E) + P_p(E)$. All of these factors have some contributions to the different ferroelectric behaviors in KNN nanotube arrays and films.³⁴ In order to take into account the geometrical dependence of P_r , the effective contact area of the capacitor was calculated and found to be $\sim 9\%$ with respect to that of a film capacitor. The normalized $2P_r$ was thus, estimated to be $37.7 \mu\text{C}/\text{cm}^2$.

The piezoresponse of an individual KNN nanotube was measured using PFM with an 11 kHz ac bias applied across the sample. Before measuring, Au film with a thickness of

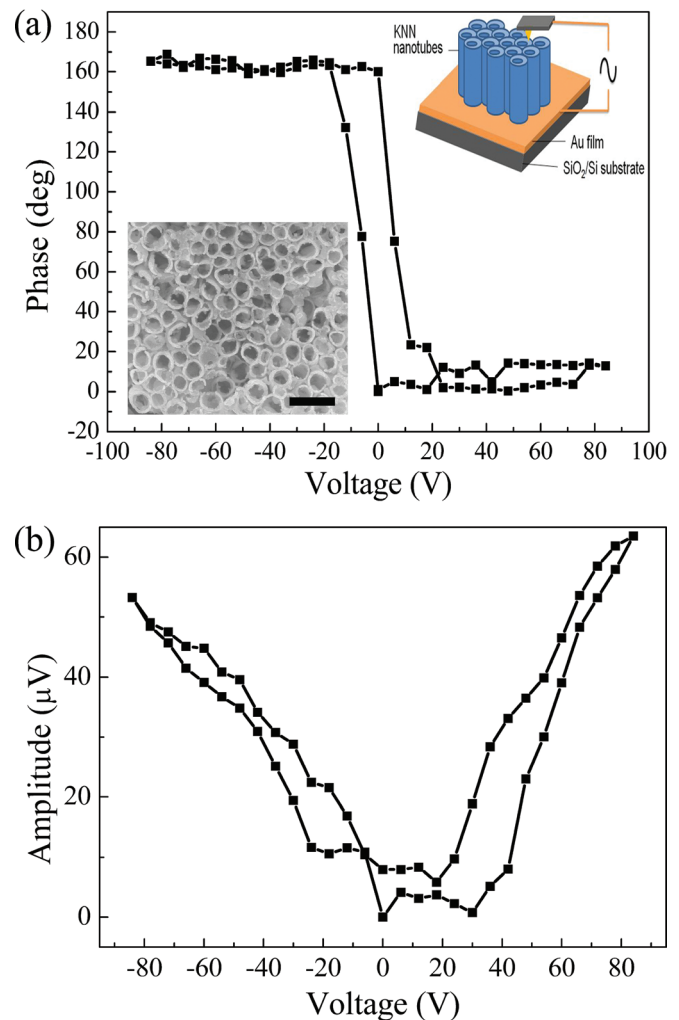


FIG. 5. (Color online) (a) Hysteresis phase loop and (b) amplitude loop of an individual KNN nanotube under axial bias voltage; the insets of Fig. 5(a) are the SEM image of top-view of nanotubes array (left, the bar is 500 nm) and the schematic drawing of the measurement configuration for PFM (right).

100 nm was coated on one side of the sample as the bottom electrode. A single KNN nanotube embedded into nanochannel of AAO template was identified by a conductive PFM tip, as shown in the insets of Fig. 5(a). The piezoresponse phase and amplitude loops are shown in Fig. 5(a) and 5(b), respectively. The square phase hysteresis loop and the classic “butterfly shape” amplitude loop reflect the piezoresponse property of the KNN nanotubes. As shown in Fig. 5(a), when changing the applied voltage from +80 to −80 V, the phase change is about 165° and smaller than 180°, which may be due to the difficulty of polarization switching in a length of 60 μm nanotube prepared in this experiment. It should be noted that there is a shift of curves to the positive bias voltage in both the phase loop and the amplitude loop. The shifts may be caused by the surface charge at the interface between the electrode and KNN, and/or the space charge stored in the AAO template walls.^{35,36} Further investigations concerning the impact brought by size and shape of KNN nanotubes such as diameter, wall thickness and aspect ratio on ferroelectric properties are in progress.

IV. CONCLUSION

In summary, KNN nanotubes were successfully fabricated using a sol-gel process combining AAO templates with pore diameters of 200 nm. The as-prepared KNN nanotubes possess a polycrystalline structure with monoclinic perovskite phase after being annealed at 700 °C for 0.5 h. The obtained nanotubes have outer diameters of about 200–250 nm, which are slightly larger than the pore diameters of the templates employed with a wall thickness of ~30–40 nm. The ferroelectric and piezoelectric properties of KNN nanotubes were investigated, which exhibit classic ferroelectric behaviors.

ACKNOWLEDGMENTS

This work was supported by the National Science Foundation of China (NSFC, Grant Nos. 90923013, 50872031, and 50902046), Research Fund for the Doctoral Program of Higher Education of China (Grant No. 20070512003), and the International Collaboration Project of Wuhan City (Grant No. 201070934340).

¹Y. M. Hu, H. S. Gu, Z. L. Hu, W. N. Di, Y. Yuan, J. You, W. Q. Cao, Y. Wang, and H. L. W. Chan, *Cryst. Growth Des.* **8**, 832 (2008).

²L. C. Samardzija, B. Malic, and M. Kosec, *Ferroelectrics* **370**, 113 (2008).

- ³J. Wang, C. Stampfer, C. Roman, W. H. Ma, N. Setter, and C. Hierold, *Appl. Phys. Lett.* **93**, 223101 (2008).
- ⁴G. Suyal, E. Colla, R. Gysel, M. Cantoni, and N. Setter, *Nano. Lett.* **4**, 1339 (2004).
- ⁵R. P. Herber and G. A. Schneider, *Appl. Phys. Lett.* **90**, 252905 (2007).
- ⁶X. D. Wang, J. Zhou, J. H. Song, J. Liu, N. S. Xu, and Z. L. Wang, *Nano. Lett.* **6**, 2768 (2006).
- ⁷C. S. Lao, Q. Kuang, Z. L. Wang, M. C. Park, and Y. L. Deng, *Appl. Phys. Lett.* **90**, 262107 (2007).
- ⁸X. D. Wang, J. H. Song, J. Liu, and Z. L. Wang, *Science* **316**, 102 (2007).
- ⁹J. Bernard, A. Benwan, and T. Rojac, *J. Am. Ceram. Soc.* **91**, 2409 (2008).
- ¹⁰Y. Zhou, M. Guo, C. Zhang, and M. Zhang, *Ceram. Int.* **35**, 3253 (2009).
- ¹¹Y. M. Hu, H. S. Gu, D. Zhou, Z. Wang, H. L. W. Chan, and Y. Wang, *J. Am. Ceram. Soc.* **93**, 609 (2010).
- ¹²Z. Wang, H. S. Gu, Y. M. Hu, K. Yang, M. Z. Hu, D. Zhou, and J. G. Guan, *Cryst. Eng. Comm.* **12**, 3157 (2010).
- ¹³C. W. Ahn, S. Y. Lee, H. J. Lee, A. Ullah, J. S. Bae, E. D. Jeong, J. S. Choi, B. H. Park, and I. W. Kim, *J. Phys. D: Appl. Phys.* **42**, 215304 (2009).
- ¹⁴E. Buixaderas, V. Bovtun, M. Kempa, M. Savinov, D. Nuzhnyy, F. Kadlec, P. Vaníek, J. Petzelt, M. Eriksson, and Z. Shen, *J. Appl. Phys.* **107**, 014111 (2010).
- ¹⁵Y. Zhao and L. Jiang, *Adv. Mater.* **21**, 3621 (2009).
- ¹⁶Z. Y. Wang, J. Hu, and M. F. Yu, *Appl. Phys. Lett.* **89**, 263119 (2006).
- ¹⁷Z. Y. Wang, A. P. Suryavanshi, and M. F. Yu, *Appl. Phys. Lett.* **89**, 082903 (2006).
- ¹⁸J. W. Hong and D. N. Fang, *J. Appl. Phys.* **104**, 064118 (2008).
- ¹⁹J. W. Hong and D. N. Fang, *Appl. Phys. Lett.* **92**, 012906 (2008).
- ²⁰G. Pilania, S. P. Alpay, and R. Ramprasad, *Phys. Rev. B* **80**, 014113 (2009).
- ²¹P. M. Rorvik, K. Tadanaga, M. Tatsumisago, T. Grande, and M. A. Einarsrud, *J. Eur. Ceram. Soc.* **29**, 2575 (2009).
- ²²R. K. Zheng, Y. Yang, Y. Wang, J. Wang, H. L. W. Chan, C. L. Choy, C. G. Jin, and X. G. Li, *Chem. Comm. (Cambridge)* 1447 (2005).
- ²³S. Singh and S. B. Krupanidhi, *Phys. Lett. A* **367**, 356 (2007).
- ²⁴F. Soderlind, P. O. Kall, and U. Helmersson, *J. Cryst. Growth* **281**, 468 (2005).
- ²⁵Y. Xu, D. W. Liu, F. P. Lai, Y. H. Zhen, and J. F. Li, *J. Am. Ceram. Soc.* **91**, 2844 (2008).
- ²⁶C. Q. Sun, *Prog. Solid State Chem.* **35**, 1 (2007).
- ²⁷F. Gao, Y. Yuan, K. F. Wang, X. Y. Chen, F. Chen, and J. M. Liu, *Appl. Phys. Lett.* **89**, 102506 (2006).
- ²⁸V. M. Kugler, F. Soderlind, D. Music, U. Helmersson, J. Andreasson, and T. Lindback, *J. Cryst. Growth* **262**, 322 (2004).
- ²⁹M. Bolmqvist, S. Khartsev, and A. Grishin, *IEEE Photonic Technol. Lett.* **17**, 1638 (2005).
- ³⁰M. Bolmqvist, J. H. Koh, S. Khartsev, and A. Grishin, *Appl. Phys. Lett.* **81**, 337 (2002).
- ³¹H. T. Huang, C. Q. Sun, T. S. Zhang, and P. Hing, *Phys. Rev. B* **63**, 184112 (2001).
- ³²T. Takeuchi, C. Capiglia, N. Balakrishnan, Y. Takeda, and H. Kageyama, *J. Mater. Res.* **17**, 575 (2002).
- ³³B. A. Hernandez, K. S. Chang, M. T. Scancella, J. L. Burris, S. Kohli, E. R. Fisher, and P. K. Dorhout, *Chem. Mater.* **17**, 5909 (2005).
- ³⁴L. W. Chen and Y. Wang, *Appl. Phys. Lett.* **75**, 4186 (1999).
- ³⁵S. Hong, J. Woo, H. Shin, J. U. Jeon, Y. E. Pak, E. L. Colla, N. Setter, E. Kim, and K. No, *J. Appl. Phys.* **89**, 1377 (2001).
- ³⁶Y. Lei, L. D. Zhang, G. W. Meng, G. H. Li, X. Y. Zhang, C. H. Liang, W. Chen, and S. X. Wang, *Appl. Phys. Lett.* **78**, 1125 (2001).